

1,2-Carbagerma-*closo*-dodecaborate as a Germanium Ligand in Coordination Chemistry – Synthesis, Structure and Reactivity

Anita Wagenpfeil,^[a] Claudia Nickl,^[a] Hartmut Schubert,^[a] Klaus Eichele,^[a] Mark A. Fox,^[b] and Lars Wesemann*^[a]

Keywords: Boranes / Cluster compounds / Germanium / Iridium / Ruthenium / Quantum chemical calculations

A much improved synthesis for the carbagerma-*closo*-dodecaborate anion $[\text{GeCB}_{10}\text{H}_{11}]^-$ is described in the form of $[\text{Bu}_3\text{NH}][\text{GeCB}_{10}\text{H}_{11}]$ (**1**). In reactions with transition metal electrophiles, three transition metal complexes $[\text{Bu}_3\text{NH}][(\text{C}_6\text{H}_6)\text{Ru}(\text{Cl})_2(\text{GeCB}_{10}\text{H}_{11})]$ (**2**), $[\text{Bu}_3\text{NH}][\text{Cp}^*\text{Ir}(\text{Cl})(\text{GeCB}_{10}\text{H}_{11})_2]$ (**3**) and $[\text{Me}_3\text{NH}][(\text{PPh}_3)_2\text{Ir}(\text{CO})-$

$(\text{GeCB}_{10}\text{H}_{11})_2]$ (**4**) with metal-germanium bonds were synthesized. The carbagermaborate anion, in the form of the salt $[\text{Et}_3\text{NH}][\text{GeCB}_{10}\text{H}_{11}]$, and the coordination compounds **2–4** were structurally characterized by single-crystal X-ray diffraction. Computations were carried out for the anions in **1–4** to aid NMR assignments.

Introduction

The coordination chemistry of germanium and tin has been a field of active research for more than 30 years.^[1] Currently, ligand development with these elements is focused on new germylene- and stannylene-type ligands based on group 14 carbene analogues.

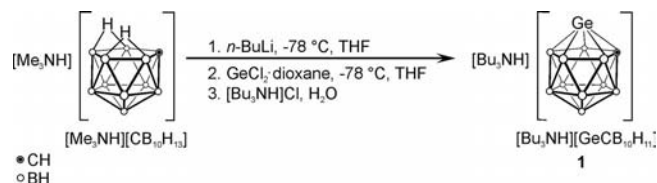
We are interested in the coordination chemistry of heteroborates and first examined the ligand abilities of the dianion stanna-*closo*-dodecaborate $[\text{SnB}_{11}\text{H}_{11}]^{2-}$ (**D** in Scheme 1).^[2–6] This twelve-vertex cluster is derived from the icosahedral *closo* cluster $[\text{B}_{12}\text{H}_{12}]^{2-}$ by isolobal replacement of a BH unit with a tin atom. We have also explored the coordination chemistry of the homologous germanium di-

anion, germa-*closo*-dodecaborate $[\text{GeB}_{11}\text{H}_{11}]^{2-}$ (**A**).^[4,7–9] We have also synthesised the new dianions $[\text{Sn}_2\text{B}_{10}\text{H}_{10}]^{2-}$ and $[\text{Ge}_2\text{B}_{10}\text{H}_{10}]^{2-}$ (**E** and **B**, respectively) where two adjacent BH units in $[\text{B}_{12}\text{H}_{12}]^{2-}$ are replaced by tin or germanium atoms.^[10] We expanded this area of heteroborates by synthesizing the new cluster monoanion $[\text{SnCB}_{10}\text{H}_{11}]^-$ (**F** in Scheme 1) where one $[\text{BH}]^-$ unit is formally replaced by an isolobal CH unit in $[\text{SnB}_{11}\text{H}_{11}]^{2-}$.^[11]

Here we present an improved synthetic procedure for the carbagerma-*closo*-dodecaborate $[\text{GeCB}_{10}\text{H}_{11}]^-$ (**C** in Scheme 1) together with new coordination compounds of this germylene-type ligand. The anion **C** was previously prepared by a two-step synthesis from the carba-*nido*-undecaborane anion $[\text{CB}_{10}\text{H}_{13}]^-$ in an overall yield of only 9%.^[12,13]

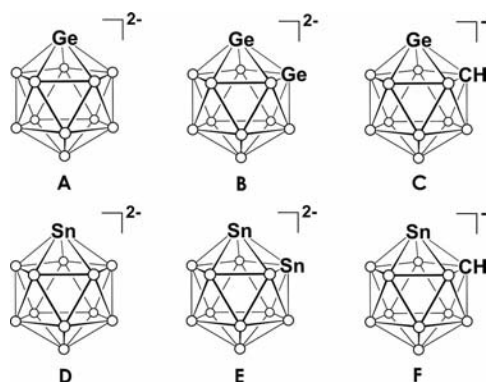
Results and Discussion

A considerably improved yield of 69% for the anion **C**, as the $[\text{Bu}_3\text{NH}]^+$ salt **1**, was obtained in one step from the carba-*nido*-undecaborane anion (Scheme 2).



Scheme 2. Formation of **1**.

After deprotonation of carba-*nido*-undecaborate $[\text{Me}_3\text{NH}][\text{CB}_{10}\text{H}_{13}]$ with BuLi, the germanium electrophile, GeCl_2 -dioxane, was added. The heteroborate was isolated by precipitation from water with salts of various counter-cations. In the case of the $[\text{Et}_3\text{NH}]^+$ salt, we were able to



Scheme 1. Group 14 heteroborates.

[a] Institut für Anorganische Chemie, Universität Tübingen, Auf der Morgenstelle 18, 72076 Tübingen, Germany
Fax: +49-7071-292436
E-mail: lars.wesemann@uni-tuebingen.de

[b] Department of Chemistry, Durham University, South Road, Durham, DH1 3LE, UK
E-mail: m.a.fox@durham.ac.uk

Table 1. Crystal and structure refinement parameters of **1–4**.

	1	2	3	4
Empirical formula	C ₇ H ₂₇ B ₁₀ GeN	C ₁₉ H ₄₅ B ₁₀ Cl ₂ GeNRu	C ₂₄ H ₆₅ B ₂₀ ClGe ₂ IrN	C ₄₆ H ₇₃ B ₂₀ Cl ₃ Ge ₂ IrN ₂ OP ₂
<i>M_r</i> [g mol ^{−1}]	305.99	640.22	956.80	1392.02
Wavelength [Å]	0.71073			
Temperature [K]	173(2)			
Crystal system	triclinic	triclinic	triclinic	monoclinic
Space group	<i>P</i> $\bar{1}$	<i>P</i> $\bar{1}$	<i>P</i> $\bar{1}$	<i>P</i> 2 ₁ / <i>c</i>
<i>Z</i>	2	2	2	4
<i>a</i> [Å]	8.2850(15)	10.9097(11)	10.0548(8)	19.8208(3)
<i>b</i> [Å]	9.1491(16)	11.4306(11)	12.6290(10)	12.7342(2)
<i>c</i> [Å]	11.2601(18)	12.0276(12)	18.0793(15)	25.8736(4)
α [°]	88.276(14)	80.573(8)	70.027(6)	90
β [°]	87.053(14)	82.956(8)	84.031(7)	102.369(1)
γ [°]	75.302(14)	83.224(8)	84.970(7)	90
<i>V</i> [Å ³]	824.4(2)	1461.1(3)	2142.7(3)	6379.0(2)
Density ρ_{calcd} [g/cm ³]	1.23	1.46	1.48	1.45
Absorption coefficient μ [mm ^{−1}]	1.84	1.74	4.57	3.23
<i>F</i> (000)	316	652	948	2776
Crystal size [mm]	0.11 × 0.10 × 0.10	0.12 × 0.10 × 0.08	0.10 × 0.09 × 0.08	0.15 × 0.13 × 0.11
θ range [°]	3.19–26.76	3.21–29.18	5.68–26.37	3.16–26.75
Index range	−10 ≤ <i>h</i> ≤ 10, −11 ≤ <i>k</i> ≤ 11, −14 ≤ <i>l</i> ≤ 14	−14 ≤ <i>h</i> ≤ 14, −15 ≤ <i>k</i> ≤ 15, −16 ≤ <i>l</i> ≤ 16	−12 ≤ <i>h</i> ≤ 12, −15 ≤ <i>k</i> ≤ 15, −22 ≤ <i>l</i> ≤ 22	−24 ≤ <i>h</i> ≤ 25, −16 ≤ <i>k</i> ≤ 16, −32 ≤ <i>l</i> ≤ 32
Reflections collected	12164	26945	29624	84891
Independent reflections/ <i>R</i> _{int}	3498/0.0707	7883/0.0554	8661/0.0771	13520/0.1097
Completeness	99.1	99.6	98.8	99.7
Absorption correction	numerical			
Max./min. transmission	0.8131/0.6703	0.7942/0.6156	0.3305/0.2137	0.3631/0.1923
Parameters/restraints	172/0	307/0	442/0	694/0
<i>R</i> ₁ / <i>wR</i> ₂ indices [<i>I</i> > 2σ(<i>I</i>)]	0.061/0.153	0.0369/0.0627	0.0390/0.0770	0.0536/0.1221
<i>R</i> ₁ / <i>wR</i> ₂ for all reflections	0.077/0.161	0.0529/0.0661	0.0521/0.0810	0.0733/0.1321
Goodness-of-fit on <i>F</i> ²	1.118	1.110	1.086	0.973
Largest diff. peak/hole [e Å ^{−3}]	1.292/−0.384	0.550/−0.854	1.363/−1.083	1.656/−1.520

isolate single crystals suitable for X-ray diffraction. The crystallographic data and refinement parameters are listed in Table 1. The molecular structure of **C**, together with selected interatomic distances, is depicted in Figure 1. This represents the first X-ray structure of a carbagermaborane anion.

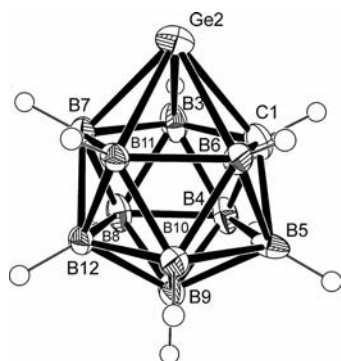


Figure 1. ORTEP plot of **C** in **1**; ellipsoids at 50% probability. Interatomic distances [Å]: Ge2–C1 2.203(5), Ge2–B11 2.190(4), Ge2–B7 2.201(5), Ge2–B3 2.203(5), Ge2–B6 2.213(5), B7–B3 1.808(7), B11–B7 1.826(6), B6–B11 1.827(6), B6–C1 1.738(6), C1–B3 1.728(6), C1–B4 1.708(6), B5–C1 1.738(6).

The Ge–C and Ge–B interatomic distances of 2.19–2.22 Å in the molecular structure of **C** are slightly shorter than the values of 2.22–2.28 Å found in crystal structures of

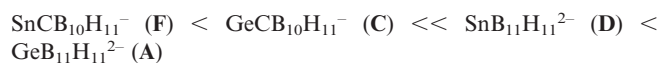
small neutral *closo*-carbagermaboranes, 1-Ge-2,4-(SiMe₃)₂-2,4-C₂B₄H₄ and 1-Ge-2,3-(SiMe₃)₂-5-GeCl₃-2,3-C₂B₄H₃.^[14] The similar Ge–C and Ge–B bond lengths determined indicate the possibility of cage disorder in the crystal, which results in difficulties in distinguishing between the CH and BH vertices.^[15] The cage ordering found in the crystal of **1** may be attributed to interactions between the acidic N–H proton in the cation and the B7–B11–B12 triangular face in **C**. The three N–H⋯B distances are 2.62, 2.63 and 2.74 Å, where the N–H bond length is normalised at 1.009 Å. These distances are shorter than the sum of the van der Waals radii for boron and hydrogen atoms. It is intriguing to see a Ge⋯Ge distance of 3.77 Å between two anions in the crystal structure as it is shorter than the sum of the van der Waals radii for the Ge atoms.

The ¹¹B{¹H} NMR spectrum for **C** was expected to show six signals (1:1:2:2:2:2), but due to peak overlap only four signals with an intensity ratio of 2:2:2:4 were detected. From the ¹¹B{¹H}–¹H heteronuclear-correlation NMR experiment, the ¹¹B NMR signals at −4.7 and −13.3 ppm couple with two signals each in the ¹H NMR spectrum. This observation indicates that the −4.7 ppm peak is assigned to the nonequivalent B9 and B12 atoms. Unfortunately, the other three ¹¹B signals could not be assigned from the ¹¹B{¹H}–¹¹B{¹H} COSY spectrum. The boron atoms adjacent to the cluster carbon atom were identified by decoupling the ¹¹B resonances selectively in the ¹³C NMR spec-

trum. The broad ^{13}C NMR peak at 59.6 ppm corresponding to the cluster carbon atom sharpens on decoupling the boron signal at -13.3 ppm. The B4,5 and B3,6 atoms are therefore assigned to the -13.3 ppm ^{11}B NMR signal.

Recently, good agreements were shown between experimental and computed geometric and NMR spectroscopic data for the tin anions **D** and **F**.^[16] Although there have been quantum mechanical investigations into boron clusters containing germanium and tin,^[5,8,17] there has been no corresponding study reported on the germanium clusters shown in Scheme 1. Here, the optimised geometry for **C** is in excellent agreement with the molecular geometry determined experimentally. The B7H and B11H vertices were calculated to have the most negative Mulliken charges of all BH vertices for **C** in agreement with the N–H...B interactions found in the X-ray crystal structure of **1**. The calculated ^{11}B NMR shifts from the optimised geometry of **C** are -3.5 (B12), -4.0 (B9), -8.0 (B7,11), -8.4 (B8,10), -13.7 (B4,5) and -13.9 (B3,6) ppm. This is in full agreement with the limited boron peak assignments determined experimentally for **C**.

Because we are interested in the coordination properties of group(IV) heteroborates, we investigated the nucleophilicity and ligand reactivity of **C**. The basicity of **C** was compared with that of other germanium and tin anions. The favourable energies on protonation of these anions at the germanium or tin atom were calculated and are listed in Table 2. The base strength for the cluster anions increases in this order:



The energies, Ge/Sn compositions and nature of the frontier orbitals from MO calculations on the anions are also listed in Table 2. Again, the order for the cluster anions with respect to the HOMO energies is found to be the same as for the base strengths. The Ge atoms show larger contributions to the HOMOs compared to the Sn atoms. Both factors indicate that the Ge cluster anions are better nucleophiles than their tin analogs.

The frontier orbitals in the cluster anions are of σ -symmetry in the HOMOs and of π -symmetry in the LUMOs at

the Ge/Sn atoms. Figure 2 shows the frontier orbitals for **C**. One exception is the π -symmetry HOMO found for **D**, which has a very similar energy value (only 0.01 eV difference) as its HOMO–2 with σ -symmetry.^[16]

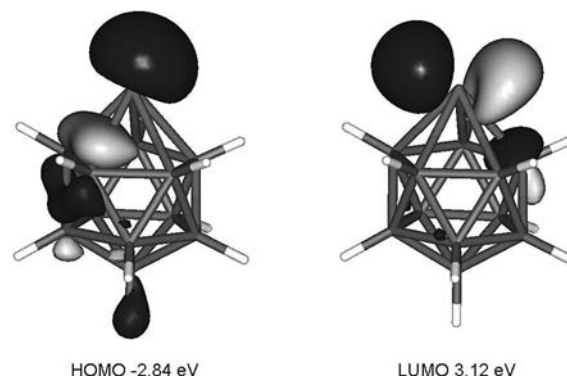


Figure 2. Computed frontier orbitals for **C**.

From Table 2, **C** has a similar basicity and nucleophilicity as GeCl_3^{-} and perhaps even more like SnCl_3^{-} . The dianion $[\text{GeB}_{11}\text{H}_{11}]^{2-}$ (**A**), on the other hand, is a stronger base and nucleophile than GeMe_3^{-} , partly due to the higher negative charge carried by **A**.

The cluster anion **C** has been reported previously to be a germanium ligand in coordination chemistry.^[13,18] Complexes with **C** as a ligand have been synthesised with the fragments $[\text{M}(\text{CO})_5]$ ($\text{M} = \text{Cr}, \text{Mo}, \text{W}$), $[\text{CpFe}(\text{CO})_2]$ and $[\text{C}_7\text{H}_7\text{Mo}(\text{CO})_3]$. Here, we present three coordination compounds with ruthenium and iridium fragments, which are the first structurally characterized examples of complexes with **C** as a ligand.

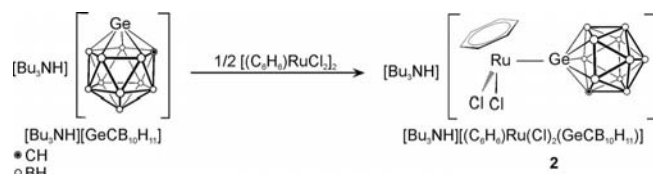
In the reaction of **C** with the (benzene)ruthenium complex $[(\text{C}_6\text{H}_6)\text{RuCl}_2]_2$, cleavage of the chlorido-bridged dimer resulted in the formation of the anion $[(\text{C}_6\text{H}_6)\text{Ru}(\text{GeCB}_{10}\text{H}_{11})\text{Cl}_2]^{-}$ as a $[\text{Bu}_3\text{NH}]$ salt (**2**) (Scheme 3). From the lack of reactivity with further equivalents of the germanium ligand we can conclude that the ligand is not a strong enough nucleophile to replace a chlorido ligand in the ruthenium complex. By comparison, the reaction of $[(\text{C}_6\text{H}_6)\text{RuCl}_2]_2$ with $[\text{SnB}_{11}\text{H}_{11}]^{2-}$ resulted in replacement of one of

Table 2. Computed data for selected germylene and stannylene anions.

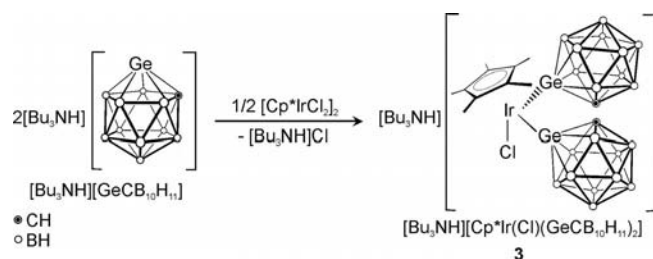
	Gas-phase proton addition ^[a] [kcal mol ⁻¹]	HOMO energy [eV]	LUMO energy [eV]	HOMO Ge/Sn %	LUMO Ge/Sn %	HOMO Ge/Sn type	LUMO Ge/Sn type
$\text{SnCB}_{10}\text{H}_{11}^{-}$ (F)	278.8	-2.87	2.45	46	84	σ	π
SnCl_3^{-}	291.7	-2.45	3.25	45	95	σ	π
$\text{GeCB}_{10}\text{H}_{11}^{-}$ (C)	293.0	-2.84	3.12	54	76	σ	π
GeCl_3^{-}	302.1	-2.37	3.50	42	81	σ	$\sigma^{[b]}$
GeF_3^{-}	343.9	-0.34	6.60	94	65	σ	π
GePh_3^{-}	363.7	-0.52	3.40	71	1	σ	$\pi^{[c]}$
GeH_3^{-}	370.3	0.64	6.90	86	74	σ	π
GeMe_3^{-}	385.3	0.88	6.69	77	82	σ	π
$\text{SnB}_{11}\text{H}_{11}^{2-}$ (D)	386.9	1.44	7.23	23	81	$\pi^{[d]}$	π
$\text{GeB}_{11}\text{H}_{11}^{2-}$ (A)	404.5	1.77	8.16	64	71	σ	π

[a] Total energy difference between the anion and its protonated form with the proton at Ge/Sn. The higher the energy value the more basic the anion. [b] LUMO+1 is $\pi(\text{Ge})$ type at 3.64 eV. [c] LUMO is $\pi(\text{phenyl})$. [d] HOMO–2 is $\sigma(\text{Ge})$ type at 1.43 eV.

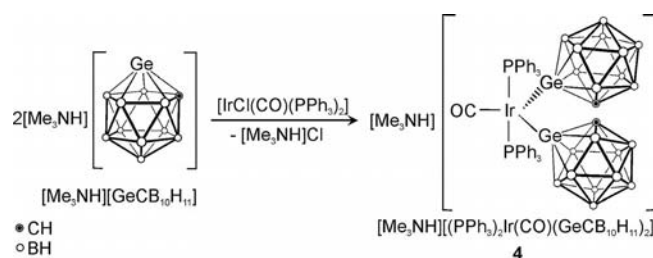
the chloride ions by the ligand.^[19] However, in the case of the iridium electrophiles, $[(\text{Cp}^*\text{IrCl}_2)_2]$ and $[\text{Ir}(\text{PPh}_3)_2\text{Cl}(\text{CO})]$, the chlorido ligand is replaced by two germanium ligands (Schemes 4 and 5). This contrasts with the lack of reaction between **F** and Vaska's complex.^[20]



Scheme 3. Formation of **2**.



Scheme 4. Formation of **3**.



Scheme 5. Reaction with Vaska's complex and formation of **4**.

The coordination compounds **2–4** were isolated in moderate yields after crystallization. Crystal structure solution and refinement data for **2–4** are listed in Table 1, and the molecular structures of the anions together with selected distances and angles are shown in Figures 3, 4 and 5.

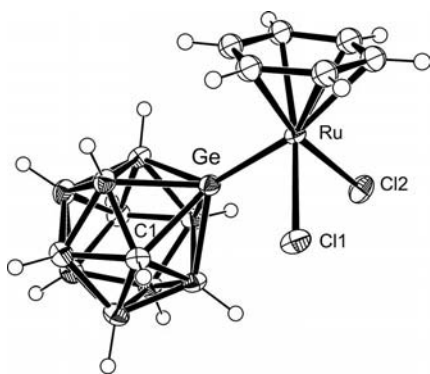


Figure 3. ORTEP plot of the anion in $[\text{Bu}_3\text{NH}][(\text{C}_6\text{H}_6)\text{Ru}(\text{Cl})_2(\text{GeCB}_{10}\text{H}_{11})]$ (**2**): ellipsoids at 50% probability. Interatomic distances [Å]: C1–Ge 2.155(3), Ru–Ge 2.3978(4), Ru–Cl1 2.3895(6), Ru–Cl2 2.4218(7).

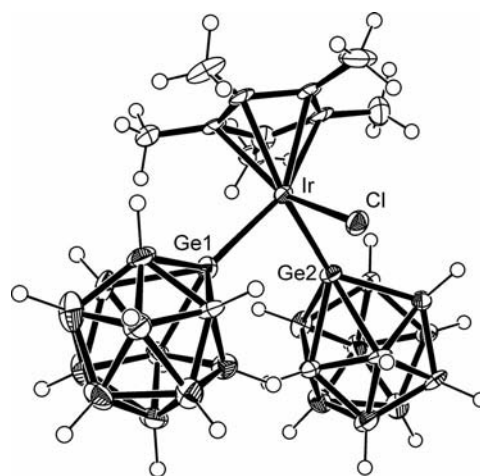


Figure 4. ORTEP plot of the anion in $[\text{Bu}_3\text{NH}][\text{Cp}^*\text{Ir}(\text{Cl})(\text{GeCB}_{10}\text{H}_{11})_2]$ (**3**): ellipsoids at 50% probability. Interatomic distances [Å] and angles [°]: Ir1–Ge1 2.3827(5), Ir1–Ge2 2.3902(6), Ir1–Cl1 2.4059(12), Ge1–C1 2.165(5), Ge1–Ir1–Ge2 92.87(2), Ge1–Ir1–Cl1 87.27(3), Ge2–Ir1–Cl1 86.76(3).

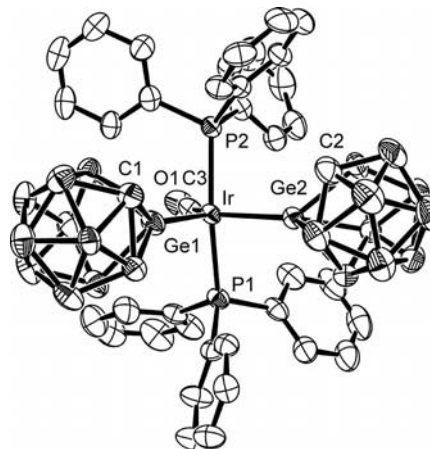


Figure 5. ORTEP plot of the anion in $[\text{Me}_3\text{NH}][(\text{PPh}_3)_2\text{Ir}(\text{CO})(\text{GeCB}_{10}\text{H}_{11})_2]$ (**4**): ellipsoids at 50% probability. Interatomic distances [Å] and angles [°]: O1–C3 1.145(8), C3–Ir1 1.860(7), Ir1–P2 2.3414(16), Ir1–P1 2.3533(16), Ir1–Ge1 2.4352(7), Ir1–Ge2 2.4408(7), C1–Ge1 2.191(7), C2–Ge2 2.197(7), O1–C3–Ir1 177.2(6), C3–Ir1–P2 82.9(2), C3–Ir1–P1 83.9(2), P2–Ir1–P1 163.66(6), C3–Ir1–Ge1 124.3(2), P2–Ir1–Ge1 97.43(4), P1–Ir1–Ge1 98.00(4), C3–Ir1–Ge2 135.6(2), P2–Ir1–Ge2 93.41(4), P1–Ir1–Ge2 89.28(5), Ge1–Ir1–Ge2 100.08(3).

In the solid state, **2** shows disorder of the benzene ligand (Figure 3). The Ru–Ge bond of 2.3978(4) Å is similar to the Ru–Ge bond lengths reported for $[\text{C}_6\text{H}_6\text{Ru}(\text{CO})(\text{GeCl}_3)_2]$ at 2.403(2) Å.^[21] Longer Ru–Ge bonds are quoted at 2.4455(4) Å for $[\text{Ru}(\text{Cl})(\text{CO})\text{-trans-}(\text{PPh}_3)_2(\text{GeMe}_3)]$ ^[22] and 2.5239(6) Å for $[\text{Ru}(\text{GeB}_{11}\text{H}_{11})(\text{MeCN})_2(\text{triphos})]$ ^[9] due to considerably different metal coordination states combined with the steric and electronic effects of the various ligands.

The Ir–Ge bonds of 2.3827(5) and 2.3902(6) in **3** are shorter than the corresponding distances of 2.4352(7) and 2.4408(7) in **4** by ca. 0.05 Å arising from the different metal coordination states (four-coordinate in **3** and five-coordinate in **4**) and different steric and electronic effects of the

noncluster ligands. The Ir–Ge values for **4** are similar to the Ir–GePh₃ and Ir–GeMe₃ bond lengths reported elsewhere: [Ir(PPh₃)₂(CO)(H)₂(GeMe₃)] 2.484(2) Å,^[23] [Ir(H)(CO)₃–(GePh₃)₂] 2.484(2) Å,^[24] [Ir(CO)₂(COD)(GePh₃)] 2.4693(2) Å (COD = cyclooctadiene),^[24] [Ir(CO)₃(GePh₃)₂][–] 2.4922(8) and 2.4932(8) Å.^[25]

The trigonal-bipyramidal geometry in **4** is also present in the analogous stanna-*closo*-dodecaborate compound, [Me₄N]₃[Ir-*trans*-(PPh₃)₂(CO)(SnB₁₁H₁₁)₂],^[6] the similar iridium complex [Et₄N][Ir-*trans*-(PPh₃)₂(CO)₂(SnB₁₁H₁₁)]^[6] and the rhodium complex [Bu₄N]₂[Rh-*trans*-(PPh₃)₂–(SnCB₁₀H₁₁)₃].^[11] Clearly, **C** behaves like **D** and **F** in favouring the equatorial positions in trigonal-bipyramidal geometries of the type ML₃(PPh₃)₂. It has been suggested that such clusters are weak π -acceptors,^[16] as shown from the LUMO of **C** in Figure 2, thus prefer the equatorial positions compared to the strong σ -donor PPh₃, but the sizes of the cluster ligands are probably also responsible. Optimization of **4** with one borato ligand in the apical position gave a geometry 3.5 kcal mol^{–1} higher in energy than the optimized *trans*-phosphane geometry.

There are several weak intra- and intermolecular contacts in the crystal structures of **2–4**. The salts **2** and **3** show N–H \cdots Cl interactions between the anion and the cation. The distances for N–H(3) \cdots Cl(1) and N–H(3) \cdots Cl(2) in **2** and N–H(1) \cdots Cl(1) in **3** are measured at 2.57, 2.55 and 2.29 Å, respectively, where the N–H bond lengths are normalised at 1.009 Å.

The clusters in the complexes **2–4** are ordered, which may be explained by the weak interactions between the acidic hydrogen atom at the cage carbon atom and an atom or ring that is electron-rich.^[15] In **2**, the intramolecular contact is 3.17 Å at C–H \cdots Cl; whereas in **3** a similar contact of 2.93 Å is found where the cage C–H bond length is normalised at 1.083 Å. There are also close C–H \cdots B contacts of 2.93 and 2.89 Å between the two cages in **3**. An intramolecular cage CH \cdots π (C₆H₅ ring centroid) contact of 2.54 Å and an intermolecular cage CH \cdots Cl interaction of 3.14 Å are found in the crystal structure of **4**. The chlorine atom in the latter interaction is from the dichloromethane solvate in the crystal.

In the ¹¹B NMR spectrum, the starting material **1** has an averaged shift of –9.6 ppm, whereas both compounds **2** and **3** have averaged shifts of –12.7 ppm. This shift towards lower frequency is expected when an electron-donating substituent is attached to a vertex in icosahedral boron clusters.^[26]

The changes in the ¹¹B NMR shifts on changing the nature of one vertex are usually significant for atoms corresponding to the neighbouring and antipodal boron atoms in icosahedral boron clusters.^[26,27] When the Ge vertex is substituted in [GeCB₁₀H₁₁][–] the ¹¹B NMR shift changes are expected to be significant for B3, B6, B7 and B11 as neighboring atoms and for B9 as the antipodal atom. As the –4.7 ppm peak is assigned to both B9 and B12 atoms in [GeCB₁₀H₁₁][–], the B9 peak value would be expected to shift significantly in compounds **2** and **3** with respect to the B12 peak. For **2**, the ¹¹B peaks observed at –5.9 and –10.6 ppm

are thus assigned to the B12 and B9 atoms, respectively; whereas for **3**, the peaks –6.3 and –10.2 ppm correspond to B12 and B9, respectively.

The gas-phase geometries of the cluster anions in **2–4** were also optimized by density functional calculations and agree very well with the molecular geometries determined by XRD. The differences in the Ge–Ir bond lengths between **3** and **4** are reproduced by computations. ¹¹B NMR shifts were computed from these geometries, and the values are in good agreement with the experimental ¹¹B NMR spectroscopic data obtained for **2–4**. The observed averaged ¹¹B NMR shifts and the B9 and B12 peak assignments discussed above are supported by the computed results.

Conclusions

The anion [GeCB₁₀H₁₁][–] is a nucleophile of moderate strength in coordination chemistry. It has similar frontier molecular orbital energies, nucleophilicity and basicity as the more widely known germylene anionic ligand [GeCl₃][–]. [GeCB₁₀H₁₁][–] is a stronger nucleophile than the homologous tin cluster [SnCB₁₀H₁₁][–] but less reactive than the stanna-*closo*-dodecaborate dianion [SnB₁₁H₁₁]^{2–} based on experimental and computational comparisons. [GeCB₁₀H₁₁][–] forms metal–germanium bonds with ruthenium and iridium complexes.

Experimental Section

General: All manipulations were carried out under dry argon by using standard Schlenk techniques. Solvents were dried and purified by established methods and stored under argon. Elemental analyses were performed at the Institut für Anorganische Chemie, Universität Tübingen, by using a Vario EL analyzer. The ESI mass spectra were recorded in positive- and negative-ion modes by using a Bruker Esquire 3000plus spectrometer equipped with an ESI interface. NMR spectra were recorded with a Bruker Avance II + 500 NMR spectrometer equipped with a 5 mm TBO probe head and operating at 500.13 (¹H), 125.76 (¹³C) and 160.46 MHz (¹¹B), a Bruker Avance II + 400 NMR spectrometer equipped with a 5 mm QNP probe head and operating at 400.13 (¹H), 100.13 (¹³C) and 161.98 (³¹P) MHz, and a Bruker DRX-250 NMR spectrometer equipped with a 5 mm ATM probe head and operating at 250.13 (¹H) and 80.25 (¹¹B) MHz. Chemical shifts are reported in δ values relative to external TMS (¹H, ¹³C), BF₃·Et₂O (¹¹B) and 85% H₃PO₄ (aq.) (³¹P). All chemicals were purchased commercially except for [Me₃NH][CB₁₀H₁₃], which was prepared according to modification of literature methods by the reduction of Me₃NCB₁₀H₁₃ with sodium metal.^[28] [(C₆H₆)RuCl₂]₂,^[29] [Cp*IrCl₂]₂^[30] and [IrCl(CO)(PPh₃)₂]^[31] were synthesized according to literature procedures.

Crystallography: X-ray data for compounds **1–4** were collected with a Stoe IPDS 2T diffractometer and were corrected for Lorentz and polarization effects and absorption by air. The programs used in this work were Stoe X-Area and the WinGX suite of programs including SHELXS and SHELXL for structure solution and refinement.^[32–37] Numerical absorption correction based on crystal-shape optimization was applied with Stoe X-Red and X-Shape. CCDC-818332 (for **1**), -818329 (for **2**), -818331 (for **3**) and -818330

(for **4**) contain the supplementary crystallographic data for this paper. These data can be obtained free of charge from The Cambridge Crystallographic Data Centre via www.ccdc.cam.ac.uk/data_request/cif.

[Bu₃NH][GeCB₁₀H₁₁] (1): A solution of [Me₃NH][CB₁₀H₁₃] (196.4 mg, 1.02 mmol) in THF (15 mL) was cooled to –78 °C, and *n*-butyllithium (1.3 mL, 3.24 mmol, 2.5 M in hexane) was added slowly. The mixture was stirred at room temperature for 3 h, and a white precipitate was formed. When butane evolution had stopped, the suspension was again cooled to –78 °C, and a solution of GeCl₂·dioxane (519.8 mg, 2.24 mmol) in THF (2 mL) was added. After warming to room temperature, the solution was stirred overnight. After removing the solvent under reduced pressure, the product was redissolved in NaOH (15 mL, 1 N), and the side products precipitate as an orange solid, which was removed by filtration. The clear filtrate was treated with [Bu₃NH]Cl to precipitate [Bu₃NH][GeCB₁₀H₁₁], which was collected by filtration and washed with plenty of water and Et₂O and dried in vacuo. Yield: 454.9 mg, 69%. MS (–)(ESI): *m/z* = 203.9 {[GeCB₁₀H₁₁]}⁺. [Bu₃NH][GeCB₁₀H₁₁] (391.95): calcd. C 40.02, H 10.08, N 3.59; found C 40.04, H 10.22, N 3.69. The [Me₃NH] salt was synthesized analogously by using [Me₃NH]⁺ as the cation. ¹H{¹¹B} NMR (CD₃CN): δ = –4.7 (2 B, B9,12), –7.5 (2 B, B7,11 or B8,10), –9.0 (2 B, B8,10 or B7,11), –13.3 (4 B, B3,6,4,5) ppm. ¹³C NMR (CD₃CN): δ = 59.6 [GeCH(BH)₁₀], 46.0 (Me₃NH) ppm. ¹H{¹¹B} NMR (CD₃CN): δ = 2.04 [1 H, GeCH(BH)₁₀], 2.51, 1.94, 1.58, 1.27 [10 H, GeCH(BH)₁₀], 2.84 (9 H, Me₃NH) ppm.

[Bu₃NH][(C₆H₆)Ru(Cl)₂(GeCB₁₀H₁₁)] (2): A solution of **1** (50 mg, 0.144 mmol) in CH₂Cl₂ (10 mL) was added by syringe to [(C₆H₆)RuCl₂] (36.3 mg, 0.072 mmol) in CH₂Cl₂ (15 mL) at room temperature. The resulting red-brown solution was stirred at room temperature for 12 h. By layering with hexane red single crystals of **2** (21.74 mg, 33.94 μmol) were obtained. Yield: 27.3%. ¹H{¹¹B} NMR (CD₂Cl₂): δ = –5.9 (1 B), –10.6 (1 B), –12.4 (4 B), –14.6 (2 B), –15.6 (2 B) ppm. ¹³C NMR (CD₂Cl₂): δ = 13.8 [(CH₃CH₂CH₂CH₂)₃NH], 20.4 [(CH₃CH₂CH₂CH₂)₃NH], 25.6 [(CH₃CH₂CH₂CH₂)₃NH], 52.8 [(CH₃CH₂CH₂CH₂)₃NH], 59.6 [GeCH(BH)₁₀], 86.0 (C₆H₆) ppm. ¹H{¹¹B} NMR (CD₃CN): δ = 2.48 [1 H, GeCH(BH)₁₀], 1.01 [9 H, (CH₃CH₂CH₂CH₂)₃NH], 1.43 [6 H, (CH₃CH₂CH₂CH₂)₃NH], 1.70 [6 H, (CH₃CH₂CH₂CH₂)₃NH], 3.05 [6 H, (CH₃CH₂CH₂CH₂)₃NH], 5.74 [6 H, (C₆H₆)], 7.89 [(CH₃CH₂CH₂CH₂)₃NH] ppm. MS (–)(ESI): *m/z* = 453.7 {[C₆H₆)Ru(Cl)(GeCB₁₀H₁₁)]⁺}. [Bu₃NH][(C₆H₆)Ru(Cl)₂(GeCB₁₀H₁₁)] (641.97): calcd. C 35.64, H 7.08, N 2.19; found C 35.65, H 7.13, N 2.24.

[Bu₃NH][Cp*Ir(Cl)(GeCB₁₀H₁₁)] (3): A solution of **1** (26.2 mg, 0.038 mmol) in CH₂Cl₂ (5 mL) was added to a solution of [Cp*IrCl₂]₂ (15 mg, 0.019 mmol) in CH₂Cl₂ (10 mL) at room temperature. The yellow solution was stirred for 12 h. Layering of this solution with hexane led to the formation of yellow single crystals of the product (11.2 mg, 0.012 mmol). Yield: 31.6%. ¹H{¹¹B} NMR (CD₂Cl₂): δ = –6.3 (1 B), –10.2 (1 B), –12.2 (4 B), –14.0 (2 B), –16.2 (2 B) ppm. ¹³C NMR (CD₃CN): δ = 13.7 [(CH₃CH₂CH₂CH₂)₃NH], 20.2 [(CH₃CH₂CH₂CH₂)₃NH], 26.0 [(CH₃CH₂CH₂CH₂)₃NH], 53.1 [(CH₃CH₂CH₂CH₂)₃NH], 55.4 [GeCH(BH)₁₀], 96.1 [(CH₃)₅C₅], 9.9 [(CH₃)₅C₅] ppm. ¹H{¹¹B} NMR (CD₃CN): δ = 2.65 [1 H, GeCH(BH)₁₀], 1.02 [9 H, (CH₃CH₂CH₂CH₂)₃NH], 1.44 [6 H, (CH₃CH₂CH₂CH₂)₃NH], 1.72 [6 H, (CH₃CH₂CH₂CH₂)₃NH], 3.10 [6 H, (CH₃CH₂CH₂CH₂)₃NH], 2.1 [15 H, (CH₃)₅C₅] ppm. MS (ESI): *m/z* = 769.1 {[Cp*Ir(Cl)(GeCB₁₀H₁₁)]⁺}. [Bu₃NH][Cp*Ir(Cl)(GeCB₁₀H₁₁)] (965.50): calcd. C 30.12, H 6.85, N 1.46; found C 30.40, H 7.08, N 1.53.

[Me₃NH][(PPh₃)₂Ir(CO)(GeCB₁₀H₁₁)] (4): To a solution of [IrCl(CO)(PPh₃)₂] (10 mg, 0.013 mmol) in CH₂Cl₂ (5 mL) was added [Me₃NH][GeCB₁₀H₁₁] (6.8 mg, 0.026 mmol) in CH₂Cl₂ (3 mL) at room temperature. The solution was stirred for 12 h. Layering of the solution with hexane led to the formation of yellow single crystals of **4**·[Me₃NH]Cl·CH₂Cl₂ (5.6 mg, 0.004 mmol). Yield: 30.8%. IR (KBr): $\tilde{\nu}$ = 2524 (BH), 1951 (CO) cm^{–1}. ¹H{¹¹B} NMR (CD₃CN): poorly resolved peaks between δ = –4.5 and –14.5 ppm. ³¹P{¹H} NMR (CD₃CN): δ = 2.8 ppm. ¹H{¹¹B} NMR (CD₃CN): 2.83 [1 H, GeCH(BH)₁₀], 7.71–7.36 (30 H, PPh₃), 2.83 (Me₃NH) ppm. ¹³C NMR (CD₃CN): δ = 135.1, 131.2, 128.5, 120.3 (PPh₃), 55.7 [GeCH(BH)₁₀], 45.8 (Me₃NH) ppm. MS (ESI): *m/z* = 1124.4 {[PPh₃)₂Ir(GeCB₁₀H₁₁)]⁺}. [Me₃NH][(PPh₃)₂Ir(CO)(GeCB₁₀H₁₁)]·[Me₃NH]Cl·CH₂Cl₂ (1360.93): calcd. C 39.66, H 5.39, N 2.01; found C 39.49, H 5.46, N 2.20.

Computations: All quantum chemical calculations were carried out at the B3LYP^{[38–40)]/6-31G*^[41] level for all atoms except Ge, Sn, Ir and Ru, which were treated with the LANL2DZ^[42] basis set by using the Gaussian 03 package.^[43] The geometries discussed here were optimized with no symmetry constraints. Electronic-structure and NMR computations were also carried out at the same level of theory. Calculated GIAO^[44] ¹¹B NMR chemical shifts were referenced to BF₃·OEt₂ for ¹¹B: δ (¹¹B) = 111.7 – σ(¹¹B).^[45] Gas-phase proton addition energies were obtained from the differences in the total energies of the anions and their optimised protonated forms. The MO diagrams and orbital contributions were generated with the aid of Gabedit^[46] and GaussSum^[47] packages, respectively. Calculated ¹¹B NMR spectroscopic data: [GeCB₁₀H₁₁][–]: δ = –3.9 (B12), –4.6 (B9), –7.2 (B7,11), –8.8 (B8,10), –13.5 (B4,5), –13.9 (B3,6), averaged shift –9.5 ppm; [Ru(C₆H₆)Cl₂GeCB₁₀H₁₁][–]: δ = –5.8 (B12), –11.8 (B9), –11.4 (B7,11), –12.5 (B8,10), –15.2 (B4,5), –15.6 (B3,6), averaged shift –12.7 ppm; [Ir(C₅Me₅)Cl(GeCB₁₀H₁₁)][–]: δ = –5.4 (B12), –10.8 (B9), –12.4 (B7,11), –12.5 (B8,10), –15.2 (B4,5), –15.5 (B3,6), averaged shift –12.7 ppm; [Ir(PPh₃)₂CO(GeCB₁₀H₁₁)][–]: δ = –4.5 (B12), –8.5 (B9), –9.6 (B7,11), –10.7 (B8,10), –14.2 (B3,6), –14.5 (B4,5), averaged shift –11.1 ppm.}

Acknowledgments

This work was supported by the Deutsche Forschungsgemeinschaft.

- [1] a) D. H. Harris, M. F. Lappert, J. B. Pedley, G. J. J. Sharp, *J. Chem. Soc., Dalton Trans.* **1976**, 945–950; b) P. J. Davidson, D. H. Harris, M. F. Lappert, *J. Chem. Soc., Dalton Trans.* **1976**, 2268–2274; c) R. D. Adams, E. Trufan, *Inorg. Chem.* **2010**, *49*, 3029–3034; d) M. Weidenbruch, *Eur. J. Inorg. Chem.* **1999**, 373–381; e) K. W. Klinkhammer, in *Chemistry of Organic Germanium, Tin and Lead Compounds* (Ed.: Z. Rappoport), Wiley, New York, **2002**, vol. 2, pp. 283–357; f) M. Veith, *Angew. Chem. Int. Ed. Engl.* **1987**, *26*, 1–14; g) J. Barrau, G. Rima, *Coord. Chem. Rev.* **1998**, *178–180*, 593–622; h) N. Tokitoh, R. Okazaki, *Coord. Chem. Rev.* **2000**, *210*, 251–277; i) S. Yao, Y. Xiong, M. Driess, *Chem. Commun.* **2009**, 6466–6468; j) O. Köhl, *Coord. Chem. Rev.* **2004**, *248*, 411–427; k) S. Nagendran, H. W. Roesky, *Organometallics* **2008**, *27*, 457–492; l) S. Inoue, M. Driess, *Organometallics* **2009**, *28*, 5032–5035; m) A. Shinohara, J. McBee, T. D. Tilley, *Inorg. Chem.* **2009**, *48*, 8081–8083; n) A. V. Zabula, F. E. Hahn, *Eur. J. Inorg. Chem.* **2008**, 5165–5179; o) S. Scharfe, F. Kraus, S. Stegmaier, A. Schier, T. F. Fässler, *Angew. Chem. Int. Ed.* **2011**, *50*, 3630–3670; p) A. Schnepf, *Eur. J. Inorg. Chem.* **2008**, 1007–1018.
- [2] For a review on stanna-closa-dodecaborate chemistry, see: T. Gädt, L. Wesemann, *Organometallics* **2007**, *26*, 2474–2481.

- [3] a) T. Marx, I. Pantenburg, L. Wesemann, *Organometallics* **2001**, *20*, 5241–5244; b) L. Wesemann, S. Hagen, T. Marx, I. Pantenburg, M. Nobis, B. Drießen-Hölscher, *Eur. J. Inorg. Chem.* **2002**, 2261–2265; c) T. Marx, B. Ronig, H. Schulze, I. Pantenburg, L. Wesemann, *J. Organomet. Chem.* **2002**, *664*, 116–122; d) T. Marx, L. Wesemann, S. Hagen, I. Pantenburg, *Z. Naturforsch. B* **2003**, *58*, 147–150; e) T. Marx, B. Mosel, I. Pantenburg, S. Hagen, H. Schulze, L. Wesemann, *Chem. Eur. J.* **2003**, *9*, 4472–4478; f) S. Hagen, L. Wesemann, I. Pantenburg, *Chem. Commun.* **2005**, 1013–1015; g) T. Gädt, L. Wesemann, *Dalton Trans.* **2006**, 328–329; h) T. Gädt, K. Eichele, L. Wesemann, *Dalton Trans.* **2006**, 2706–2713; i) T. Gädt, B. Grau, K. Eichele, I. Pantenburg, L. Wesemann, *Chem. Eur. J.* **2006**, *12*, 1036–1045; j) T. Gädt, F. M. Schappacher, R. Pöttgen, L. Wesemann, *Inorg. Chem.* **2007**, *46*, 2864–2869; k) M. Kirchmann, K. Eichele, L. Wesemann, *Organometallics* **2008**, *27*, 6029–6031; l) M. Kirchmann, K. Eichele, F. M. Schappacher, R. Pöttgen, L. Wesemann, *Angew. Chem. Int. Ed.* **2008**, *47*, 963–966; m) M. Kirchmann, K. Eichele, L. Wesemann, *Inorg. Chem.* **2008**, *47*, 5988–5991; n) M. Kirchmann, T. Gädt, K. Eichele, L. Wesemann, *Eur. J. Inorg. Chem.* **2008**, 2261–2265; o) H. Schubert, L. Wesemann, *Organometallics* **2010**, *29*, 4906–4913; p) M. Hornung, L. Wesemann, *Eur. J. Inorg. Chem.* **2010**, 2949–2955.
- [4] H. Schubert, J.-A. Dimmer, F.-R. Kühle, K. Eichele, L. Wesemann, *Inorg. Chem.* **2011**, *50*, 664–670.
- [5] a) S. Hagen, H. Schubert, C. Maichle-Mössmer, I. Pantenburg, F. Weigend, L. Wesemann, *Inorg. Chem.* **2007**, *46*, 6775–6784; b) T. Gädt, L. Wesemann, *Z. Anorg. Allg. Chem.* **2007**, *633*, 693–699; c) S. Hagen, I. Pantenburg, F. Weigend, C. Wickleder, L. Wesemann, *Angew. Chem. Int. Ed.* **2003**, *42*, 1501–1505; d) T. Marx, L. Wesemann, S. Dehnen, I. Pantenburg, *Chem. Eur. J.* **2001**, *7*, 3025–3032; e) T. Marx, L. Wesemann, S. Dehnen, *Z. Anorg. Allg. Chem.* **2001**, *627*, 1146–1150.
- [6] M. Kirchmann, S. Fleischhauer, L. Wesemann, *Organometallics* **2008**, *27*, 2803–2808.
- [7] J.-A. Dimmer, H. Schubert, L. Wesemann, *Chem. Eur. J.* **2009**, *15*, 10613–10619.
- [8] J.-A. Dimmer, M. Hornung, F. Weigend, L. Wesemann, *Dalton Trans.* **2010**, *39*, 7504–7512.
- [9] J.-A. Dimmer, L. Wesemann, *Eur. J. Inorg. Chem.* **2011**, 235–240.
- [10] a) D. Joosten, I. Pantenburg, L. Wesemann, *Angew. Chem. Int. Ed.* **2006**, *45*, 1085–1087; b) C. Nickl, D. Joosten, K. Eichele, C. Maichle-Mössmer, K. W. Törnroos, L. Wesemann, *Angew. Chem. Int. Ed.* **2009**, *48*, 7920–7923.
- [11] D. Joosten, I. Weissinger, M. Kirchmann, C. Maichle-Mössmer, F. M. Schappacher, R. Pöttgen, L. Wesemann, *Organometallics* **2007**, *26*, 5696–5701.
- [12] L. J. Todd, A. R. Burke, H. T. Silverstein, J. L. Little, G. S. Wikholm, *J. Am. Chem. Soc.* **1969**, *91*, 3376–3377.
- [13] G. S. Wikholm, L. J. Todd, *J. Organomet. Chem.* **1974**, *71*, 219–224.
- [14] a) N. S. Hosmane, J. Yang, K.-J. Lu, H. Zhang, U. Siriwardane, M. S. Islam, J. L. C. Thomas, J. A. Maguire, *Organometallics* **1998**, *17*, 2784–2796; b) U. Siriwardane, M. S. Islam, J. A. Maguire, N. S. Hosmane, *Organometallics* **1988**, *7*, 1893–1895.
- [15] M. A. Fox, A. K. Hughes, *Coord. Chem. Rev.* **2004**, *248*, 457–476.
- [16] M. A. Fox, T. B. Marder, L. Wesemann, *Can. J. Chem.* **2009**, *87*, 63–71.
- [17] a) M. Zhang, Y. Zhao, *Theochem.* **2001**, *545*, 105–110; b) F. A. Kiani, M. Hofmann, *Dalton Trans.* **2006**, 686–692.
- [18] T. Yamamoto, L. J. Todd, *J. Organomet. Chem.* **1974**, *67*, 75–80.
- [19] S. Fleischhauer, L. Wesemann, to be published.
- [20] I. Heber, Dissertation, Universität Tübingen, **2010**.
- [21] L. Y. Y. Chan, W. A. G. Graham, *Inorg. Chem.* **1975**, *14*, 1778–1781.
- [22] B. Marciniak, H. Ławicka, M. Majchrzak, M. Kubicki, I. Kownacki, *Chem. Eur. J.* **2006**, *12*, 244–250.
- [23] N. A. Bell, F. Glockling, M. L. Schneider, H. M. M. Shearer, M. D. Wibley, *Acta Crystallogr., Sect. C: Cryst. Struct. Commun.* **1984**, *40*, 625.
- [24] R. D. Adams, E. Trufan, *Organometallics* **2010**, *29*, 4346–4353.
- [25] J. M. Allen, W. W. Brennessel, C. E. Buss, J. E. Ellis, M. E. Minyaev, M. Pink, G. F. Warnock, M. L. Winzenburg, V. G. Young Jr., *Inorg. Chem.* **2001**, *40*, 5279–5284.
- [26] S. Heřmánek, *Chem. Rev.* **1992**, *92*, 325–362.
- [27] For examples of ^{11}B NMR antipodal effects in icosahedral boron clusters, see: a) A. R. Siedle, G. M. Bodner, A. R. Garber, D. C. Beer, L. J. Todd, *Inorg. Chem.* **1974**, *13*, 2321–2324; b) F. Teixidor, C. Viñas, R. W. Rudolph, *Inorg. Chem.* **1986**, *25*, 3339–3345; c) A. S. Batsanov, P. A. Eva, M. A. Fox, J. A. K. Howard, A. K. Hughes, A. L. Johnson, A. M. Martin, K. Wade, *J. Chem. Soc., Dalton Trans.* **2000**, 3519–3525; d) C. Viñas, G. Barberà, J. M. Oliva, F. Teixidor, A. J. Welch, G. M. Rosair, *Inorg. Chem.* **2001**, *40*, 6555–6562; e) L. A. Boyd, W. Clegg, R. C. B. Copley, M. G. Davidson, M. A. Fox, T. G. Hibbert, J. A. K. Howard, A. Mackinnon, R. J. Peace, K. Wade, *Dalton Trans.* **2004**, 2786–2799; f) J. G. Planas, C. Viñas, F. Teixidor, M. E. Light, M. B. Hursthouse, H. R. Ogilvie, *Eur. J. Inorg. Chem.* **2005**, 4193–4205; g) M. A. Fox, R. J. Peace, W. Clegg, M. R. J. Elsegood, K. Wade, *Polyhedron* **2009**, *28*, 2359–2370.
- [28] W. H. Knoth, J. L. Little, J. R. Lawrence, F. R. Scholer, L. J. Todd, *Inorg. Synth.* **1968**, *11*, 33–41.
- [29] R. A. Zelonka, M. C. Bard, *Can. J. Chem.* **1972**, *50*, 3063–3072.
- [30] R. G. Ball, W. A. G. Graham, D. M. Heinekey, J. K. Hoyano, A. D. McMaster, B. M. Mattson, S. T. Michel, *Inorg. Chem.* **1990**, *29*, 2023–2025.
- [31] M. J. Burk, R. H. Crabtree, *Inorg. Chem.* **1986**, *25*, 931–932.
- [32] X-AREA 1.26, Stoe & Cie GmbH, Darmstadt, Germany, **2004**.
- [33] L. F. Farrugia, *J. Appl. Crystallogr.* **1999**, *32*, 837–838.
- [34] G. M. Sheldrick, *SHELXS 97, Program for the Solution of Crystal Structures*, Göttingen, Germany, **1997**.
- [35] G. M. Sheldrick, *SHELXS 97, Program of the Crystal Structure Refinement*, Göttingen, Germany, **1997**.
- [36] X-RED 1.26, Data Reduction for STAD4 and IPDS, Stoe & Cie, Darmstadt, **1996**.
- [37] X-SHAPE 2.05, Crystal optimization for absorption correction, Stoe & Cie, Darmstadt, Germany, **1996**.
- [38] A. D. Becke, *J. Chem. Phys.* **1993**, *98*, 5648–5652.
- [39] C. Lee, W. Yang, R. G. Parr, *Phys. Rev. B* **1988**, *37*, 785–789.
- [40] P. J. Stephens, F. J. Devlin, C. F. Chabalowski, M. J. Frisch, *J. Phys. Chem.* **1994**, *98*, 11623–11627.
- [41] a) G. A. Petersson, M. A. Al-Laham, *J. Chem. Phys.* **1991**, *94*, 6081–6090; b) G. A. Petersson, A. Bennett, T. G. Tensfeldt, M. A. Al-Laham, W. A. Shirley, J. Mantzaris, *J. Chem. Phys.* **1988**, *89*, 2193–2218.
- [42] a) T. H. Dunning Jr., P. J. Hay, in *Modern Theoretical Chemistry* (Ed.: H. F. Schaefer III), Plenum, New York, **1976**, vol. 3, p. 1–28; b) P. J. Hay, W. R. Wadt, *J. Chem. Phys.* **1985**, *82*, 270–283; c) W. R. Wadt, P. J. Hay, *J. Chem. Phys.* **1985**, *82*, 284–298; d) P. J. Hay, W. R. Wadt, *J. Chem. Phys.* **1985**, *82*, 299–310.
- [43] M. J. Frisch, G. W. Trucks, H. B. Schlegel, G. E. Scuseria, M. A. Robb, J. R. Cheeseman, J. A. Montgomery Jr., T. Vreven, K. N. Kudin, J. C. Burant, J. M. Millam, S. S. Iyengar, J. Tomasi, V. Barone, B. Mennucci, M. Cossi, G. Scalmani, N. Rega, G. A. Petersson, H. Nakatsuji, M. Hada, M. Ehara, K. Toyota, R. Fukuda, J. Hasegawa, M. Ishida, T. Nakajima, Y. Honda, O. Kitao, H. Nakai, M. Klene, X. Li, J. E. Knox, H. P. Hratchian, J. B. Cross, C. Adamo, J. Jaramillo, R. Gomperts, R. E. Stratmann, O. Yazyev, A. J. Austin, R. Cammi, C. Pomelli, J. W. Ochterski, P. Y. Ayala, K. Morokuma, G. A. Voth, P. Salvador, J. J. Dannenberg, V. G. Zakrzewski, S. Dapprich, A. D. Daniels, M. C. Strain, O. Farkas, D. K. Malick, A. D.

- Rabuck, K. Raghavachari, J. B. Foresman, J. V. Ortiz, Q. Cui, A. G. Baboul, S. Clifford, J. Cioslowski, B. B. Stefanov, G. Liu, A. Liashenko, P. Piskorz, I. Komaromi, R. L. Martin, D. J. Fox, T. Keith, M. A. Al-Laham, C. Y. Peng, A. Nanayakkara, M. Challacombe, P. M. W. Gill, B. Johnson, W. Chen, M. W. Wong, C. Gonzalez, J. A. Pople, *Gaussian 03*, Revision C.02, Gaussian, Inc., Wallingford CT, **2004**.
- [44] a) R. Ditchfield, *Mol. Phys.* **1974**, 27, 789–807; b) C. M. Rohling, L. C. Allen, R. Ditchfield, *Chem. Phys.* **1984**, 87, 9–15; c) K. Wolinski, J. F. Hinton, P. Pulay, *J. Am. Chem. Soc.* **1990**, 112, 8251–8260.
- [45] a) C. E. Willans, C. A. Kilner, M. A. Fox, *Chem. Eur. J.* **2010**, 16, 10644–10648; b) M. Bühl, P. v. R. Schleyer, *J. Am. Chem. Soc.* **1992**, 114, 477–491; c) T. Onak, M. Diaz, M. Barfield, *J. Am. Chem. Soc.* **1995**, 117, 1403–1410.
- [46] A. R. Allouche, *Gabedit 2.1.0*, CNRS et Université Claude Bernard Lyon1, **2007**; available at <http://gabedit.sourceforge.net>.
- [47] N. M. O'Boyle, A. L. Tenderholt, K. M. Langner, *J. Comput. Chem.* **2008**, 29, 839–845.

Received: March 25, 2011
Published Online: June 28, 2011